SCIENCE CHINA
Life Sciences

•RESEARCH PAPER•

February 2021 Vol.64 No.2: 294–310
https://doi.org/10.1007/s11427-020-1780-x

Roles of *FERONIA-like receptor* genes in regulating grain size and quality in rice

Long Wang[1,2,3†], Dandan Wang[2†], Zhuhong Yang[1,3†], Shun Jiang[2], Jianing Qu[2], Wei He[1,2], Zhenming Liu[2], Junjie Xing[3], Youchu Ma[2], Qinlu Lin[2*] & Feng Yu[1,3*]

[1]*State Key Laboratory of Chemo/Biosensing and Chemometrics, and Hunan Province Key Laboratory of Plant Functional Genomics and Developmental Regulation, College of Biology, Hunan University, Changsha 410082, China;*
[2]*National Engineering Laboratory for Rice and By-product Deep Processing, Central South University of Forestry and Technology, Changsha 410004, China;*
[3]*State Key Laboratory of Hybrid Rice, Hunan Hybrid Rice Research Center, Changsha 410125, China*

Received May 5, 2020; accepted July 17, 2020; published online August 20, 2020

Grain yield and quality are critical factors that determine the value of grain crops. In this study, we analyzed the functions of 12 FERONIA-like receptor (FLR) family members in rice and investigated their effects on grain size and quality. We found that FLR1, FLR2 and FLR8 negatively regulated grain size, and FLR15 positively regulated grain size. *flr1* mutants had a higher cell number and an accelerated rate of grain filling compared to wild-type plants, which led to grains with greater widths. A mechanism underlying the regulation of grain size by FLR1 is that FLR1 is associated with OsRac1 Rho-like GTPase, a positive regulator of grain size. Regarding grain quality, the *flr1* mutant had a higher percentage of chalkiness compared with wild-type plants, and seeds carrying mutations in *flr3* and *flr14* had endosperms with white floury cores. To elucidate the possible mechanism underlying this phenomenon, we found that *FLR1* was constitutively expressed during endosperm development. RNA-seq analysis identified 2,367 genes that were differentially expressed in the *flr1* mutant, including genes involved in starch and sucrose metabolism and carbon fixation. In this study, we identified the roles played by several *FLR* genes in regulating grain size and quality in rice and provided insights into the molecular mechanism governing the *FLR1*-mediated regulation of grain size.

FLR, chalkiness, seed size, grain quality, OsRac1

Citation: Wang, L., Wang, D., Yang, Z., Jiang, S., Qu, J., He, W., Liu, Z., Xing, J., Ma, Y., Lin, Q., et al. (2021). Roles of *FERONIA-like receptor* genes in regulating grain size and quality in rice. Sci China Life Sci 64, 294–310. https://doi.org/10.1007/s11427-020-1780-x

INTRODUCTION

Rice (*Oryza sativa* L.) is one of the most important cereal crops worldwide and is consumed by more than half of the world's population. In recent years, consumers have become increasingly selective regarding the flavor of rice, and breeding programs have focused on generating high-yield and high-quality rice breeds (Zhang, 2007). The grain yield of rice is influenced by three major factors: the number of grains per panicle, the number of panicles per plant and the 1,000-grain weight (Sakamoto and Matsuoka, 2008). Grain weight is determined by grain size, which is measured by grain width, grain length and grain thickness. Grain size is regulated by several signaling pathways, including the ubiquitin-proteasome pathway, the G-protein signaling pathway, the mitogen-activated protein kinase (MAPK) signaling pathway, and the phytohormone pathway. The MAPK sig-

†Contributed equally to this work
*Corresponding authors (Qinlu Lin, email: linql0403@126.com; Feng Yu, email: feng_yu@hnu.edu.cn)

naling pathway is composed of three protein kinases: MAPK kinase kinase (MKKK), MAPK kinase (MKK), and MAPK (Xu and Zhang, 2015). In rice, OsMKKK10, OsMKK4 and OsMAPK6 act as kinase cascades to control grain size (Guo et al., 2018; Xu et al., 2018), where OsMKKK10 phosphorylates OsMKK4 and OsMKK4 subsequently phosphorylates OsMAPK6, thereby leading to the positive regulation of gain size by OsMAPK6 (Xu et al., 2018). A recent study found that OsRac1, a member of ROP GTPases, regulates grain size by interacting with OsMAPK6 (Zhang et al., 2019). OsRac1 exhibits a GTP-bound activated form and a GDP-bound inactivated form, which are regulated by either exchange factors (GEFs) or NLR family R protein (Kawano et al, 2010; Akamatsu et al, 2013). These two forms of OsRac1 have different binding capacities with distinct proteins (Kawano et al, 2010; Duan et al., 2010), suggesting that different forms of OsRac1 have different roles.

Starch, protein and lipids are the main nutrients contained in rice grains. Among these nutrients, starch accounts for more than 70% of the rice endosperm; therefore, starch synthesis is essential for grain quality. Starch is synthesized from sucrose and is stored in amyloplasts through such enzymes as granule-bound starch synthase (GBSS) that synthesizes amylose, as well as soluble starch synthases (SSs), branching enzymes (BEs), and debranching enzymes (DBEs), which synthesize amylopectin (Hannah and James, 2008; Nakamura, 2018). Plants carrying loss-of-function copies of these genes have floury, white-core or chalky endosperm. For example, *SS* mutants have chalky endosperm, where the starch granules are loosely packed and irregularly shaped (Hirose and Terao, 2004; Zhang et al., 2011). In addition to these enzymes, other genes have also been implicated in regulating starch synthesis. *FLO2* encodes a nuclear-localized TPR-binding protein and interacts with bHLH transcription factors to regulate the expression of starch synthesis-associated genes, and *flo2* mutants have white and floury endosperm (She et al., 2010). *FLO6* encodes a C-terminal carbohydrate-binding module 48 (CBM48) domain protein and regulates starch synthesis and starch granule formation (Peng et al., 2014). *FLO7* regulates amyloplast development within the peripheral endosperm, and *flo7* mutants have floury white regions in the peripheral parts of the grain (Zhang et al., 2016). *Abnormal flower and grain1* (*afg1*) mutants showed decreased total starch and amylose contents (Yu et al., 2020). Although significant advances have been made in identifying factors that regulate grain size and quality, how plants perceive external environmental signals and endogenous hormones and modulate the functions of these genes to regulate grain size and quality has not been determined.

Receptor-like kinases (RLKs) enable plants to sense changes in environmental and endogenous signals and constitute the largest receptor family in plants. In general, an RLK protein consists of an extracellular receptor domain, a transmembrane domain and an intracellular Ser/Thr kinase domain. The extracellular receptor domain senses extracellular signals and phosphorylates downstream targets to activate various physiological pathways (Luo and Liu, 2018). *Catharanthus roseus* receptor-like kinase (*Cr*RLK1L) is an essential RLK-type obtained from *Catharanthus roseus* that has a unique extracellular domain (Schulze-Muth et al., 1996). There are 17 *Cr*RLK1L members in *Arabidopsis*, such as FERONIA (FER), THESEUS1 (THE1), HERCULES1 (HERK1), and HERCULES2 (HERK2) (Nissen et al., 2016). FER is a highly conserved receptor kinase that is involved in cell elongation. For example, *fer* mutants are defective in cell elongation and have smaller leaves, shorter root hairs and fewer epidermal hairs (Guo et al., 2009; Duan et al., 2010; Mao et al., 2015), indicating that FER positively regulates cell elongation in certain vegetative tissues. In contrast, FER inhibits cell elongation in other cell types. Seeds carrying mutations in *FER* have a higher level of cell elongation and larger seeds; this phenotype is mediated by the GEF-ROP/Rac network (Yu et al., 2014). Different RAPID ALKALINIZATION FACTOR (RALF) peptides serve as extracellular ligands for FER that each has varied functions (Ge et al., 2019). LRE (LORELEI) and LLG1 (LRE-like GPI-APs), which act as chaperones/coreceptors for FER, function in combination with FER after LLG1/LER-FER perceives different RALF peptides (Haruta et al., 2014; Stegmann et al., 2017; Xiao et al., 2019; Ge et al., 2019). Additionally, the RALF1-FER pathway affects mRNA translation and alternative splicing to modulate RNA metabolism (Zhu et al., 2020; Wang et al., 2020a; Wang et al., 2020b). FER also regulates carbon (C) and nitrogen (N) utilization by interacting with the E3 ubiquitin ligase ATL6, which decreases 14-3-3 protein levels and reduces sensitivity to a high C/N ratio (Xu et al., 2019). Furthermore, FER serves as a regulator of starch metabolism by interacting with glyceraldehyde-3-phosphate dehydrogenase (GAPC), and *FER* loss-of-function mutants have higher starch content that mimics the phenotype of *gapc1/2* mutants (Yang et al., 2015). These studies demonstrate the importance of FER in metabolism and other basic cellular functions.

At present, the function of FERONIA-like receptor (FLR) family members in rice has been determined in the context of fertility, growth and stress response. For example, the expression of some *OsCrRLK1Ls* is induced by drought and is regulated by circadian rhythms (Nguyen et al., 2015). *FLR1*/*DWARF AND RUNTISH SPIKELET1* (*DRUS1*) and *FLR2*/*DRUS2* are two members of the FLR family that are involved in the reproduction, development and growth of rice (Li et al., 2016; Pu et al., 2017). In addition, two *FLR* genes (*FLR2* and *FLR11*) negatively regulate the rice blast fungus response (Yang et al., 2020; Huang et al., 2020). The FLR family member ruptured pollen tube (RUPO) is specifically

expressed in rice pollen and mediates K^+ homeostasis, which is necessary for pollen tube growth and male gamete transmission (Liu et al., 2016). Therefore, it may be meaningful to systematically study the functions of a single FLR role in rice to achieve sustainable crop improvement. Furthermore, most of the findings obtained for this family concern only one member of *Arabidopsis*, FER. Therefore, further research is warranted to determine whether such components have been conserved in a common pathway throughout plant evolution. In this study, we examined grain size and quality in *flr* mutants and found that FLR family members play different roles in regulating grain size and quality. In particular, we determined that FLR1 affects grain size by interacting with OsRac1 and induces changes in the expression of genes involved in starch metabolism during grain quality regulation.

RESULTS

Function of *FLR* genes in grain size

FLR1 and FLR2 had the highest protein sequence homology to *At*FER from *Arabidopsis* (Figure S1A and B in Supporting Information); therefore, we used previously generated *flr1* and *flr2* transfer DNA (T-DNA) mutants (Li et al., 2016) to test whether *FLR* genes affect grain size. In addition, we obtained six independent *FLR1* overexpression (*FLR1-OE*) transgenic lines and seven independent *FLR2* overexpression (*FLR2-OE*) transgenic lines. We confirmed increased expression levels of the target genes in two lines for *FLR1* (*OE-7* and *OE-8*) and two lines for *FLR2* (*OE-4* and *OE-7*) (Figure S2A and B in Supporting Information). We compared seed sizes and 1,000-grain weights among wild type (WT), *flr1*, *flr2*, *FLR1-OE-7*, *FLR1-OE-8*, *FLR2-OE-4* and *FLR2-OE-7* plants, and we found that grain width was significantly greater in the *flr1* mutant than in the WT (+14.28%), and the grain width was narrower in the *FLR1-OE* lines than in the WT (*OE-7*, −8.57%; *OE-8*, −9.14%) (Figure 1A and B). Grain length was higher in the *flr2* mutants compared with WT (+13.04%), but the grain sizes for the *FLR2-OE* transgenic lines and the WT line were similar (Figure 1A–D). The length-width ratio was lower in the *flr1* mutant and higher in *FLR1-OE* and *flr2* mutant compared with the WT (Figure 1E). Compared with the WT, the 1,000-grain weight of *flr1* (+7.76%) and *flr2* (+7.92%) were significantly higher, and the 1,000-grain weight was significantly lower in the *FLR1-OE* transgenic lines (OE-7, −9.64%; OE-8, −12.69%) (Figure 1F). Taken together, these results suggest that *FLR1* and *FLR2* regulate grain size, with *FLR1* regulating grain width and *FLR2* regulating grain length. In addition, the increased grain weight observed in the *flr1* and *flr2* mutants may be attributable to larger grain size.

Our findings demonstrated the importance of *FLR1* and *FLR2* in regulating grain size; therefore, we attempted to determine the role played by all *FLR* family genes in regulating grain size. CRISPR/Cas9 (clustered regularly interspaced short palindromic repeats/CRISPR-associated protein 9) was used to generate mutants of 16 *FLR* family genes in Nipponbare (NPB) (Figure S3 in Supporting Information), and 12 *flr* homozygous mutant seeds were obtained. For each *FLR* gene, we generated two independent mutant lines that were identified using PCR (Figure S4 in Supporting Information). We were unable to obtain mutants for *FLR4* and *FLR6*, and the *flr9* and *flr13* mutants were sterile. The seed size phenotypes of *flr1* and *flr2* mutants obtained through CRISPR-Cas9 were consistent with the *flr1* and *flr2* T-DNA mutants (Figure 2A and B). Furthermore, grain length and width were observed to be significantly higher in the *flr8* mutant lines than in the WT and were significantly reduced in *flr15* (Figure 2A–D). To confirm the mutant phenotypes, we generated two independent *FLR8-OE* lines (Figure S2C in Supporting Information) and found that the grain size of the *FLR8-OE* lines was lower than that of the WT (Figure 2E and F). All other *flr* CRISPR-Cas9 mutant lines had similar grain length and width phenotypes as WT (Figure 2A and B). These results indicated that two FLR genes, *FLR8* and *FLR15*, have opposite functions in regulating grain size, with *FLR8* negatively regulating grain size and *FLR15* positively regulating grain size.

Most receptor protein kinases affect plant growth and development (Morris and Walker, 2003); for instance, the *flr1* and *flr2* mutants are shorter than the wild-type plants, and the grain yield per plant is lower in both *flr1* and *flr2* mutants (Li et al., 2016). Thus, we investigated the plant height and fertility of *flr8* and *flr15* mutant lines that had grain phenotypes. The plant height and setting percentage of *flr8* were similar to those of the WT (Figure S5A–C in Supporting Information). However, *flr15* mutants were shorter and had lower fertility than the WT (Figure S5D–F in Supporting Information). Thus, *FLR15* was determined to regulate the grain size, growth and development of rice plants, while *FLR8* appeared to be involved primarily in regulating seed size.

FLR1 modulates grain size by regulating cell expansion and division in the spikelet

We investigated FLR1 as a detailed example to further characterize how *FLR* regulates grain width, and we performed a time course measurement of the grain width of filled grains in the *flr1* mutant and the WT. Grain width is influenced by the developing endosperm, and we found that the growth rate of the width was higher in *flr1* than in WT, especially from day after flowering (DAF) 0 to DAF 15 (Figure 3A and B). Therefore, *FLR1* may alter seed plumpness by increasing the rate of grain filling.

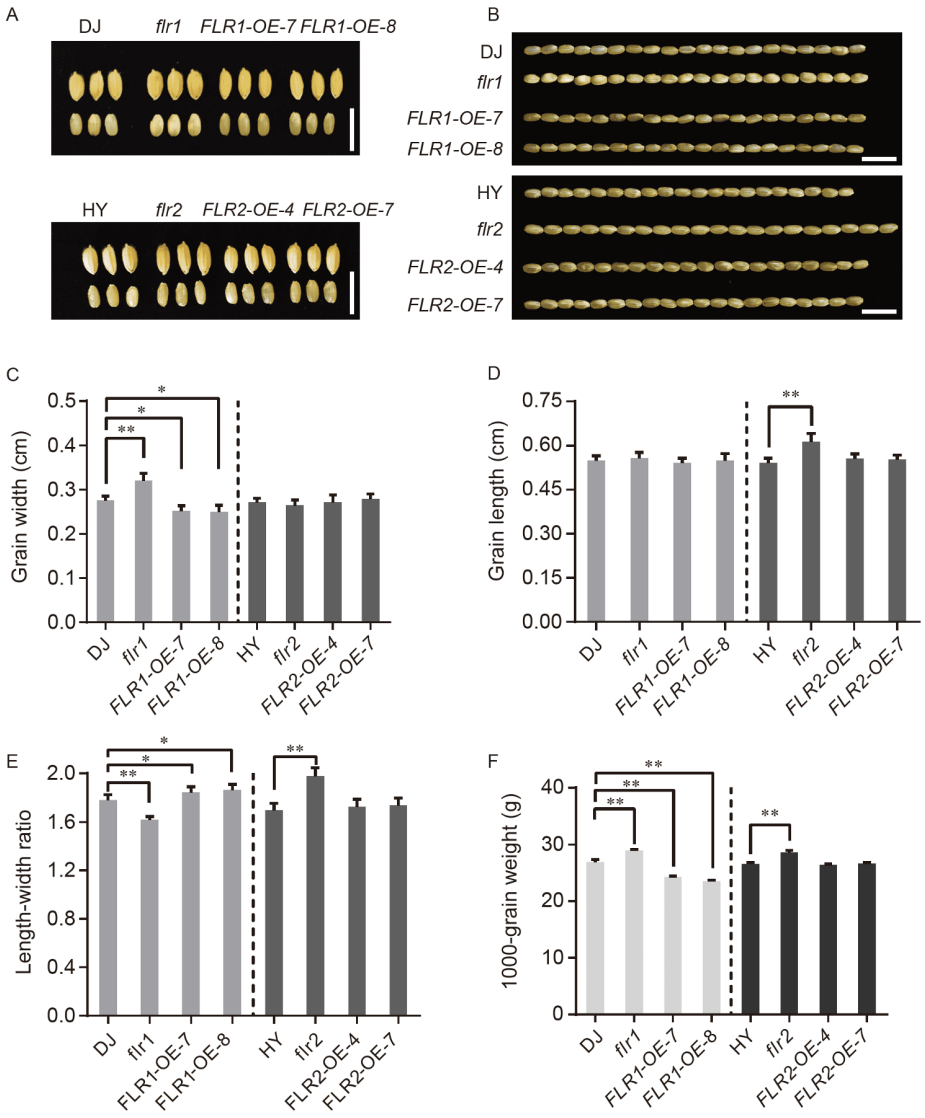

Figure 1 Grain size in WT, *flr1*, *flr2* and overexpression lines. A, Grain size of *flr1*, *FLR1-OE-7* and *FLR1-OE-8* plants in the Dongjin (DJ) background, and *flr2*, *FLR2-OE-4* and *FLR2-OE-8* transgenic plants in the Hwayoung (HY) background. Scale bar, 1 cm. B, Grain length of experimental genotypes. Scale bar, 1 cm. C–E, Statistical analyses of grain width (C), grain length (D) and length/width ratio (E) for DJ, *flr1* (n=257), *FLR1-OE-7* (n=133), *FLR1-OE-8* (n=144), HY (n=111), *flr2* (n=182), *FLR2-OE-4* (n=169) and *FLR2-OE-7* (n=176). The error bars represent the standard deviation (SD). **, P<0.01; *, P<0.05; one-way ANOVA with Tukey's test. The results were repeated with three batches of seeds. F, 1,000-grain weight of different genotypes. The error bars represent the SD of three independent experiments. **, P<0.01, one-way ANOVA with Tukey's test.

Spikelet hulls can influence final grain size (Li et al., 2019), and the final size of a spikelet hull is primarily affected by two factors: cell size and cell number. We first compared the spikelet width of Dongjin (DJ, WT) and *flr1* mutants before grain filling. The spikelet width was significantly higher in the *flr1* mutant than in the WT (+9.96%, Figure S6A and B in Supporting Information). Cross-sections of the central parts of spikelet hulls before grain filling showed that parenchyma cell size and cell number were significantly higher in *flr1* mutants than in the WT (Figure S6C–F in Supporting Information). Similarly, scanning electron microscopy demonstrated that the average glume outer surface cell length was greater in *flr1* seeds than in WT seeds (Figure 3C and D). In contrast, *FLR1-OE-8* and the WT had similar cell lengths (Figure 3C and D). In addition, the average glume outer surface cell number of *flr1* mutants was greater than that of WT (Figure 3C and E), and *FLR1-OE-8* had fewer cells than WT (Figure 3C and E). Taken together, these results indicate that changes in both cell expansion and cell division underlie the large grain size observed in the *flr1* mutants.

FLR1 interacts with OsRac1 to control grain size

We attempted to identify the downstream interacting partner (s) of FLR1 using a yeast two-hybrid (Y2H) screen to elu-

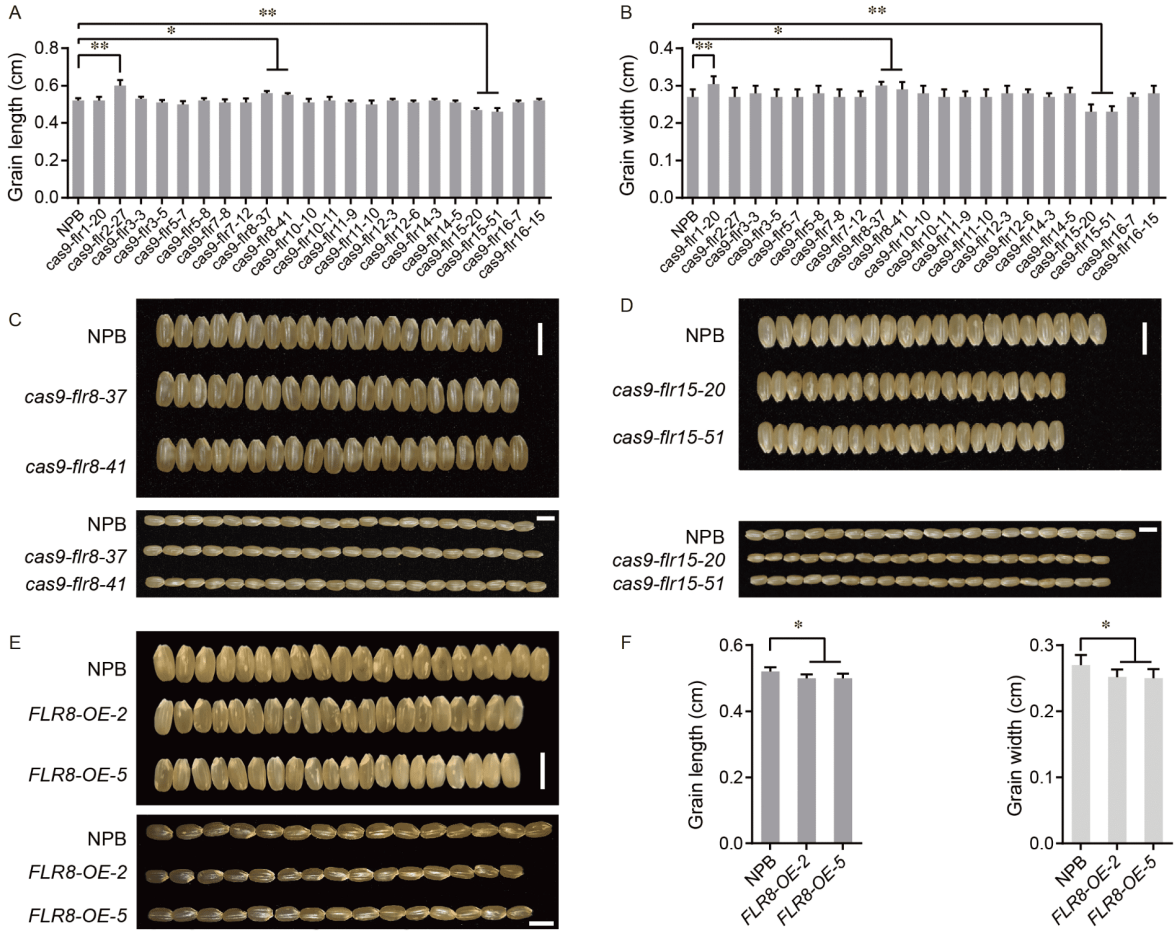

Figure 2 Functional analyses of *FLR* genes in grain size regulation. A and B, Statistical analyses of grain length (A) and grain width (B) in WT and *flr* CRISPR-Cas9 lines. The *flr* CRISPR-Cas9 lines and WT were grown in the same location and mature seeds were harvested at the same time. Error bars indicate SD (n=100). *, P<0.05; **, P<0.01; one-way ANOVA with Tukey's test. The results were repeated using three batches of seeds. C–E, Grain morphology of Nipponbare (NPB) and *flr8* CRISPR-Cas9 lines (C), *flr15* CRISPR-Cas9 lines (D) and *FLR8-OE* transgenic lines (E). The images were taken from one representative replicate, scale bar, 0.5 cm. F, Comparisons of grain length, grain width between WT (Nipponbare) and *FLR8-OE* transgenic lines. Error bars indicate SD (n=150). *, P<0.05, one-way ANOVA with Tukey's test.

cidate the mechanisms by which *FLR1* regulates grain size. Rice complementary DNA (cDNA) libraries were screened using the FLR1 kinase domain as bait, and this approach yielded an interaction with OsRac1 (Table S1 in Supporting Information), a protein that regulates cell division and grain size in rice (Zhang et al., 2019). Using Y2H, we confirmed that full-length OsRac1 interacted with the FLR kinase domain (FLR-KD) (Figure 4A). OsRac1 also interacted with FLR8 and FLR15 but did not interact with FLR2 (Figure 4A). The interaction between the FER kinase domain and AtGEF1 served as a positive control (Duan et al., 2010). Next, we conducted coimmunoprecipitation (Co-IP) assays using coexpressed OsRac1-FLAG and FLR1-GFP in the human cell line HEK293T. We employed HEK293T cells to easily express full-length FLRs and OsRac1 *in vivo* and to minimize potential background interactions between these proteins and other plant proteins (Wang et al., 2016). FLR1 also interacted with OsRac1 in HEK293T cells (Figure S7A in Supporting Information). In addition, we obtained two independent *OsRac1-OE* lines with a Flag tag (Figure S7B in Supporting Information) and confirmed the interaction between FLR1 and OsRac1 *in vivo* through Co-IP assays (Figure 4B). Furthermore, we obtained *OsRac1* CRISPR-Cas9 mutant seeds (Figure S7C in Supporting Information) and confirmed that *OsRac1* positively regulates grain size (Figure S7D and E in Supporting Information), which is consistent with the findings obtained in previous work (Zhang et al., 2019). OsRac1 has a GTP-bound activated form and a GDP-bound inactivated form (Yang and Fu, 2007). To elucidate the mechanisms by which FLR1-OsRac1 regulates grain size, we performed two-hybrid yeast assays. The FLR1 kinase domain interacted with a constitutively active form of OsRac1 (CA-OsRac1) but not with a dominant-negative form of OsRac1 (DN-OsRac1; Figure S7F in Supporting Information). The pulldown assay showed that the active GTP form of OsRac1 has greater affinity towards FLR1 than does the inactive GDP form of OsRac1 (Figure 4C). We hypothesized that FLR1 might bind with the more

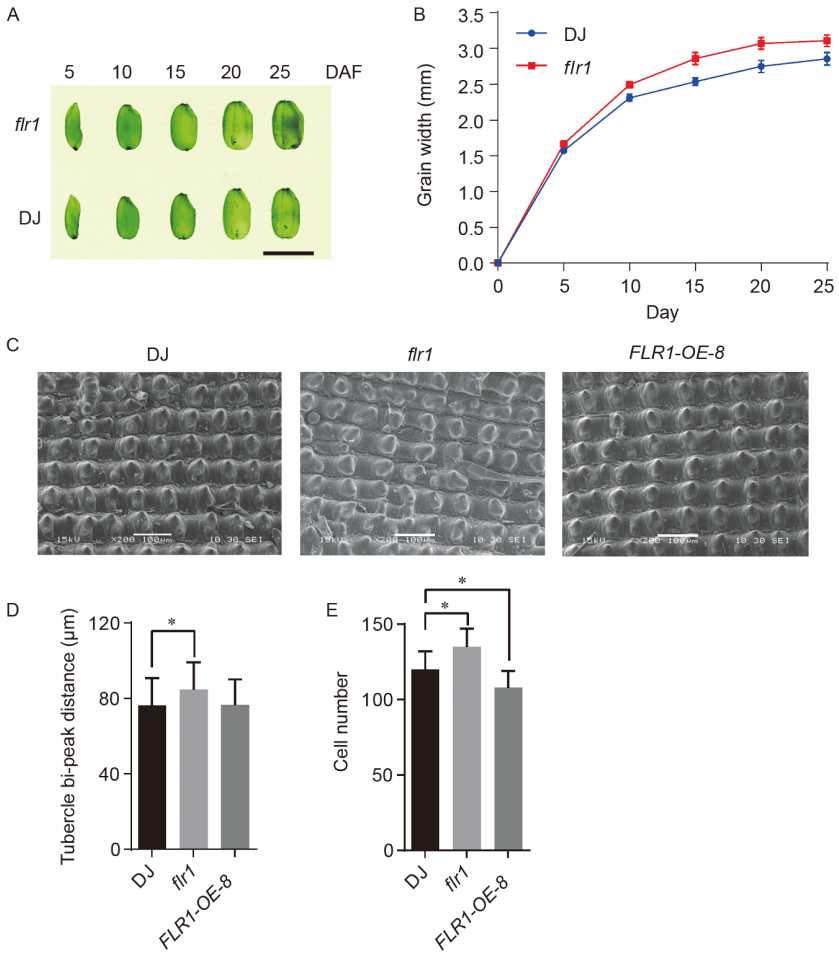

Figure 3 Roles of FLR1 in grain filling rate and cell division. A, The filling of WT (DJ) and *flr1* mutant grains at 5, 10, 15, 20, 25 DAF. Scale bar, 0.5 mm, representative images are from one of three independent experiments. B, Time course of endosperm width in WT (DJ, n=50) and the *flr1* mutants (n=35). Error bars represent SD. Three independent experiments were conducted with similar results. C, Scanning electron micrographs of the outer surfaces of DJ, *flr1* and *FLR1-OE-8* spikelet hulls. Scale bar, 100 μm. D and E, Statistical analyses of the average tubercle bi-peak distances (D) and cell number (E) on the outer surfaces of the mature spikelet hulls. Error bars represent SD (n=9). *, P<0.05; one-way ANOVA with Tukey's test.

activated OsRac1 on the cell membrane, which would lead to less activated OsRac1 being released from the cell membrane to interact with downstream effectors (such as OsMAPK6) as a means of regulating grain size (Zhang et al., 2019). ROP-INTERACTIVE CRIB MOTIF-CONTAINING PROTEIN 1 (AtRIC1), which binds specifically to the GTP-bound form of OsRac1, was used to analyze the activity of OsRac1 in different plant genotypes. The level of activated OsRac1 increased in the *flr1* mutant relative to wild-type plants but decreased in *FLR1-OE-8* plants (Figure 4D). In contrast, activated OsRac1 decreased in the *flr15* mutant compared to the wild type line (Figure S7G in Supporting Information). Taken together, these data indicate that FLR1 partially regulates grain size by interacting with OsRac1.

Roles of *FLR* genes in regulating grain quality

To analyze the effects of *FLR* family genes on grain quality, we compared the percentages of grains with chalkiness in the *flr1*, *flr2*, *FLR1-OE*, *FLR2-OE* and WT lines. The grains of *flr1* mutants were chalkier than those of the WT. There were no obvious differences in grain chalkiness among the *flr2*, *FLR1-OE*, *FLR2-OE* and WT lines (Figure 5A–C). Furthermore, scanning electron microscopy (SEM) of the grains demonstrated that the *flr1* endosperm was packed with small, loose, and irregular polyhedral starch grains, whereas WT and *FLR1-OE* endosperm contained tightly packed, large, and irregular polyhedral starch grains (Figure 5D). In addition, the starch grain morphologies of the *flr2* mutant, *FLR2-OE* and WT lines were similar (Figure 5D). To determine the cytological differences that underlie the starch grain phenotype in *flr1*, we observed semithin sections of mature endosperm under a microscope. Under I_2-KI treatment, amylose is stained blue, and amylopectin is stained purple. Mature WT endosperm had amyloplasts filled with densely packed polyhedral starch granules in the central region

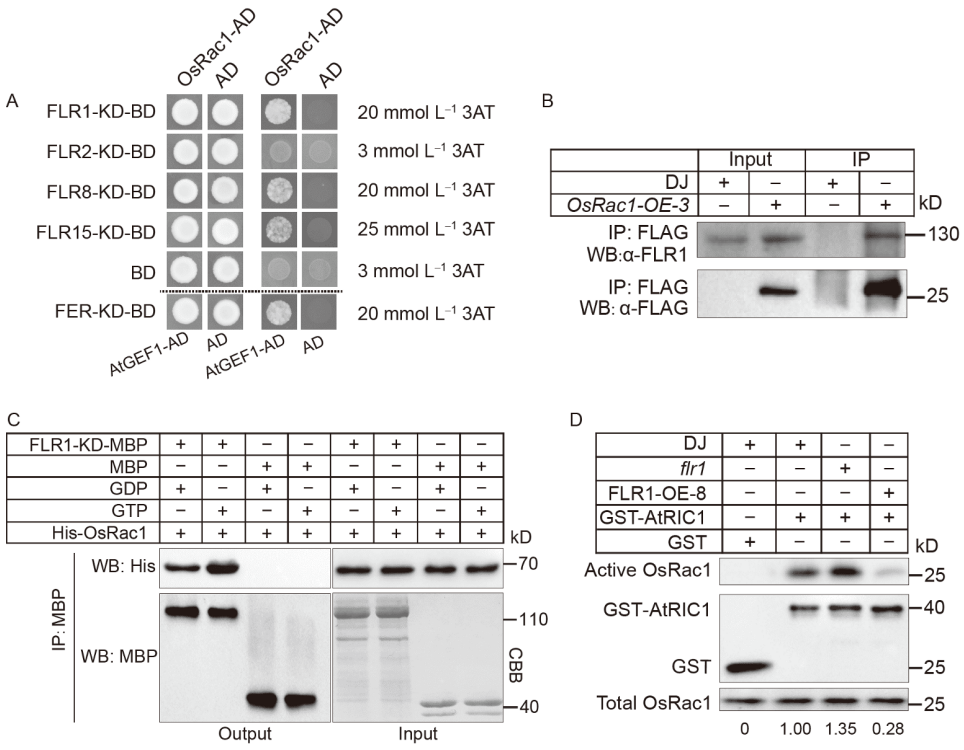

Figure 4 FLR1 interacts with OsRac1. A, Y2H analyses of the interaction between OsRac1 and FLR1, FLR2, FLR8 and FLR15's kinase domains. SD/-Ade/-Leu selection medium (left) and SD/-Ade/-Leu/-His selection medium containing different 3-AT concentration (right) were used to screen for yeast growth. Experiments were repeated three times. B, Co-IP assays. The immunoprecipitated FLR1 and coimmunoprecipitated OsRac1 were recognizedusing anti-FLAG and anti-FLR1 antibodies, respectively. OsRac1 was fused with a Flag tag in the *OsRac1-OE-3* plant. The input lanes are indicated. Three independent experiments were conducted with similar results. C, *In vitro* binding assays of OsRac1 and FLR1 with GTP, GDP. Purified MBP-tagged FLR1 kinase domain, MBP protein and His-tagged OsRac1 were subjected to this assay with MBP resin. The FLR1-MBP and His-OsRac1 were detected with anti-MBP and anti-His antibody, respectively. The MBP input protein was visualized with Coomassie Brilliant Blue (CBB). D, Pull down of active OsRac1. GST-AtRIC1 protein and GST bead were used for DJ, *flr1* mutant and *FLR1-OE-8* plants. Total OsRac1 and active OsRac1 were detected with anti-OsRac1 antibody, GST-AtRIC1 and GST protein were detected with anti-GST antibody. The active OsRac1/total OsRac1 ratio is displayed below the gel. The band ratio was measured with ImageJ. Three independent experiments were conducted with similar results in B–D.

(Figure S8A in Supporting Information). However, in contrast, the *flr1* mutant had more amyloplasts with smaller and more disordered starch granules in the central region of the endosperm (Figure S8A and B in Supporting Information). Meanwhile, compared to the WT, the central region of the *FLR1-OE* endosperm had amyloplasts with larger and more densely packed starch granules (Figure S8A and B in Supporting Information). Taken together, these results suggest that *FLR1* may play a role in starch packing density and starch granule size.

We next analyzed the chalkiness of *flr* CRISPR-Cas9 mutants and found that *flr3* and *flr14* mutants exhibited white-core floury endosperm (Figure 6A–C). We also generated *FLR3-OE* and *FLR14-OE* plants (Figure S2D and E in Supporting Information) and found that the chalkiness phenotype was similar for *FLR3-OE*, *FLR14-OE* and the WT (data not shown). The other *FLR* family mutants had similar grain chalkiness as the WT (Figure 6A). These results indicate that *FLR3* and *FLR14* may be involved in grain filling, resulting in the white-core floury endosperm observed in the mutants.

FLR1 affects the accumulation of starch and protein in seeds

We next analyzed the effect of *FLR1* and *FLR2* on the storage of starch and proteins in seeds. Starch content was higher in *flr1* mutants (+7.59%) compared to WT, while starch content was slightly reduced in *FLR1-OE-7* (−4.11%) and *FLR1-OE-8* lines (−3.93%) (Figure 7A). Meanwhile, starch content was similar for *flr2* (65.38%), *FLR2-OE-4* (65.61%), *FLR2-OE-7* (65.12%) and the WT (65.78%) (Figure 7A). Amylose content (AAC) was higher in *flr1* (20.55%) but lower in *FLR1-OE-7* (16.32%) and *FLR1-OE-8* (16.35%) compared to the WT (18.10%) (Figure 7B). Compared to WT, total protein content was reduced by 1.23% in *flr1* mutants and increased by 1.02% and 1.04% in *FLR1-OE-7* and *FLR1-OE-8*, respectively (Figure 7C). These results highlighted the role of *FLR1* in starch and protein content. This function may affect the edibility of rice; therefore, we analyzed the pasting properties (thought to have an effect on the edibility of rice) of the WT, *flr1*, *FLR1-OE-7* and *FLR1*-OE-8 lines using a

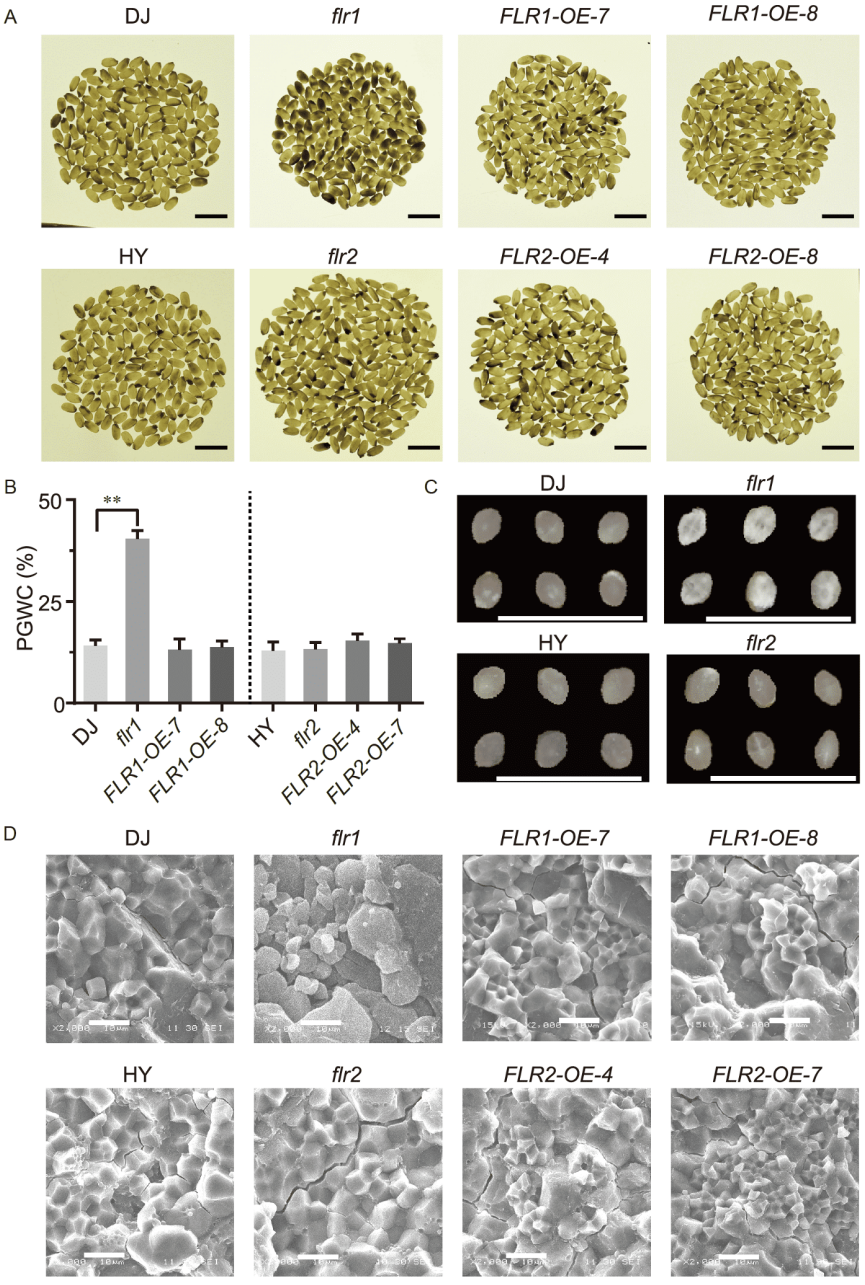

Figure 5 Phenotypic analyses of grains in WT, *flr1*, *flr2* and overexpression lines. A, Mature grains in a white light background. Scale bar, 1 cm. B, Percentage of grains with chalkiness for each different genotype. The error bars represent the SD of three biological replicates. **, $P<0.01$; one-way ANOVA with Tukey's test. C, Transverse sections of representative DJ, *flr1,* HY and *flr2* grains. Scale bar, 1 cm. D, Scanning electron microscopy images of transverse sections of DJ, *flr1*, *FLR1-OE-7*, *FLR1-OE-8*, HY, *flr2*, *FLR2-OE-4* and *FLR2-OE-7* grains. Scale bar, 10 μm. All experiments were repeated three times with similar results.

Rapid Visco Analyzer (RVA), a method for assessing the pasting properties of starch (Shafie et al., 2016). Compared to the WT, *flr1* had lower peak viscosity (PV), hold viscosity (HV) and final viscosity (FV) (Shafie et al., 2016), while *FLR1-OE-7* and *FLR1-OE-8* had higher values of PV, HV and FV (Figure 7D). These results suggest that *FLR1* may regulate starch content, protein content and starch pasting properties, whereas *FLR2* does not affect these parameters.

FLR1 expression pattern during endosperm development

In our recent studies, we employed qRT-PCR to analyze the expression patterns of *FLR* family genes in various organs (Yang et al., 2020). To further understand the role of *FLR1* on grain quality and size, we analyzed the expression pattern of *FLR1* in various parts of the rice plant, especially during endosperm development. A Pro_{OsFLR1}*:GUS* transgenic line

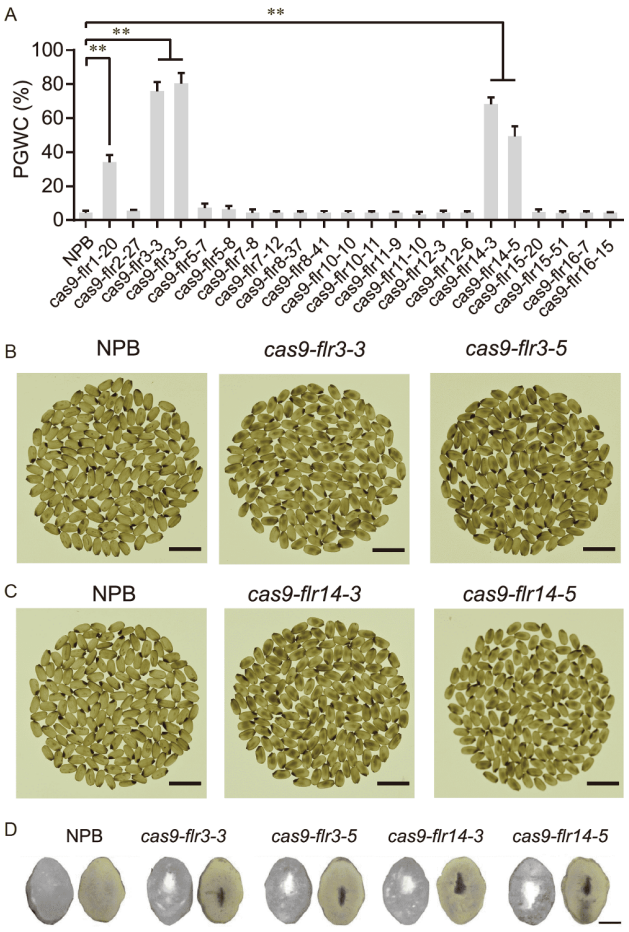

Figure 6 Phenotypic analyses of grains in different *flr* CRISPR-Cas9 lines. A, Percentage of grain with chalkiness (PGWC) of different genotypes (n=3). The error bars represent the SD of three biological replicates. **, P<0.01; one-way ANOVA with Tukey's test. B and C, Grains of Nipponbare, *flr3* CRISPR-Cas9 lines (B) and *flr14* CRISPR-Cas9 lines (C) in white light background. The images are representative of three replicates. Scale bar, 1 cm. D, Morphology of endosperms in WT and *flr* CRISPR-Cas9 lines. *flr3* CRISPR-Cas9 and *flr14* CRISPR-Cas9 endosperms had white-core floury endosperm in the center. Scale bar, 1 mm. The experiments were replicated three times.

was generated using a histochemical β-glucuronidase (GUS) reporter gene controlled by the *FLR1* promoter, and strong GUS staining was observed in the root, stem and panicle, but only weak levels of staining were observed in the leaf (Figure 8A). These results were consistent with previous research (Li et al., 2016; Pu et al., 2017). Next, we analyzed the expression of *FLR1* during endosperm development and found that *FLR1* expression increased from DAF 6 to DAF 12 and decreased from DAF 12 to DAF 18 (Figure 8A and B). To analyze protein accumulation in the endosperm, we generated an antibody against FLR1. The antibody was able to detect endogenous FLR1 in the WT but not in the *flr1* mutant (Figure S2F in Supporting Information). Western blot (WB) analysis was conducted on protein extracts from different endosperm developmental stages, and we found that FLR1 protein levels increased from DAF 6 to DAF 12 and decreased from DAF 12 to DAF 18 (Figure 8C). In summary, we observed that *FLR1* is constitutively expressed during endosperm development, and its expression level peaks during the middle stages (DAF 12) of endosperm development.

FLR1 affects the expression levels of starch biosynthesis-related genes in the developing endosperm

FLR1 expression was highest during DAF 12, and RNA-sequencing (RNA-seq) experiments were performed using DAF 12 of WT and *flr1* to determine the roles played by *FLR1* during endosperm development. We generated over 6.5 Gb of clean bases. The Q30 was higher than 93.2% for each sample (Figure S9A in Supporting Information). More than 98.46% of reads could be properly mapped to the MSU rice genome (Figure S9B in Supporting Information), and a comparison of the mapped reads to the gene model (MSU Rice Genome Annotation Project, Release 7) revealed that approximately 99% of the reads mapped to exonic regions (Figure S9C in Supporting Information). There were 1,699 upregulated genes and 668 downregulated genes in the *flr1* mutant compared to the WT (fold change>1.5; P<0.05) (Figure 9A and B, Table S2 in Supporting Information). Gene Ontology (GO) term enrichment analysis of differentially expressed genes (DEGs) revealed that the expression of genes involved in metabolic processes, the generation of metabolites and energy and the response to stress were different in the *flr1* mutant compared to the WT (Figure 9C). This finding indicated that *FLR1* might regulate metabolic processes during endosperm development. Furthermore, the DEGs were enriched in the Kyoto Encyclopedia of Genes and Genomes (KEGG) pathways for carbon metabolism, photosynthesis, biosynthesis of amino acids, carbon fixation, starch and sucrose metabolism and fatty acid degradation (Figure 9D, Table S2 in Supporting Information). Among the 20 DEGs in the starch and sucrose metabolism pathway, three important starch synthase-related genes, *SSII-2* (LOC_Os02g51070), *AMYC2* (LOC_Os06g49970) and *SPS4* (LOC_Os08g20660), were upregulated in the *flr1* mutant, which is consistent with the higher starch content and higher amylose content observed in the mutant grains (Figure 9E). Among the 16 DEGs involved in carbon fixation, 14 genes were upregulated in *flr1*, which indicates that the *FLR1* mutation accelerates the carbon fixation process (Figure 9E).

Although there was no enrichment in protein synthesis pathway genes, biosynthesis of the amino acid pathway was enriched in *flr1* mutants compared with WT (Figure S9D in Supporting Information). This enrichment may underlie the differences in protein levels in the *flr1* mutants. To validate the RNA-seq data and compare the expression patterns of other important genes involved in starch synthesis that may

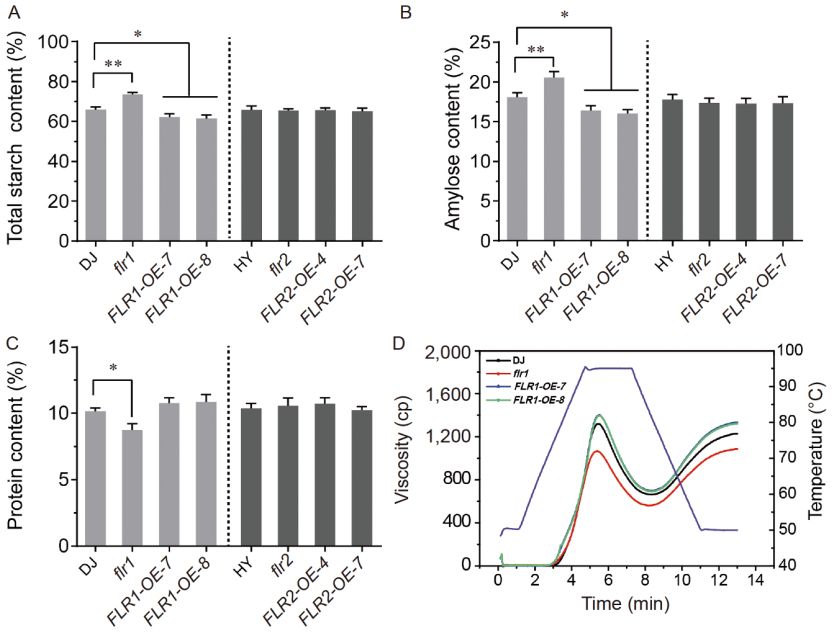

Figure 7 Comparisons of total starch, amylose and protein content in mature seeds of different genotypes. A–C, Contents of total starch (A), amylose (B), protein (C) in DJ, *flr1*, *FLR1-OE-7*, *FLR1-OE-8*, HY, *flr2*, *FLR2-OE-4* and *FLR2-OE-8* lines. Error bars represent the SD of three biological replicates. **, $P<0.01$; one-way ANOVA with Tukey's test. D, Pasting properties of DJ, *flr1*, *FLR1-OE-7* and *FLR1-OE-8* grains analyzed using Rapid Visco Analyzer (RVA). Similar results were obtained in three independent replicates.

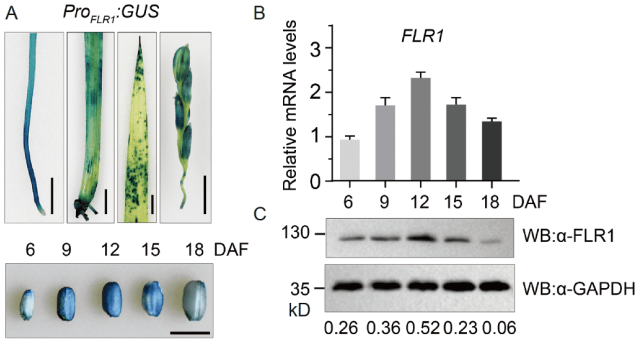

Figure 8 Expression pattern of FLR1. A, GUS activity in root, stem, leaf, panicle and developmental stages of the endosperms in *Pro$_{OsFLR1}$:GUS* plants. Scale bar, 5 mm. Representative images are from one of three replicates. Scale bar, 0.5 cm. B, Expression levels of *FLR1* in the developing endosperms of the WT. *ACTIN* was used as the internal control. Values are mean±SD. The experiment was repeated three times. C, Western blot analyses of FLR1 in the developing WT endosperms. GAPDH was used as a loading control, at least three biological replicates were performed.

be regulated by *FLR1*, we measured the expression levels of starch biosynthesis-related genes. We first confirmed that *SSII-2*, *AMYC2*, and *SPS4* were upregulated in *flr1* mutants (Figure 9F), and we found that *AGPL2* (ADP-glucose pyrophosphorylase large subunit 2, LOC_Os03g52460), a gene that encodes a protein that catalyzes the synthesis of ADP-glucose, was also upregulated in the *flr1* mutants (Figure 9G). However, the expression patterns of several genes involved in starch synthesis were similar for *flr1* mutants and the WT (Figure 9G), such as *SSIIa* (starch synthase II a, LOC_Os06g12450), *Wx* (LOC_Os06g04200), *FLO4* (floury endosperm 4, LOC_Os05g33570) and *FLO6* (LOC_Os03g48170). Taken together, these results suggest that *FLR1* affects the expression of starch biosynthesis-related genes and carbon fixation-related genes in the developing endosperm, which are essential for establishing starch content in rice grains.

FLR1 regulates both grain size and grain quality. To analyze whether the regulation of grain quality by FLR1 is the result of its role in grain size, we analyzed the chalkiness of OsRac1 CRISPR-Cas9 mutant and overexpression lines compared with wild-type plants and found no difference among them (Figure S10A in Supporting Information). In addition, the mRNA expression of *SSII-2*, *AMYC2*, *SPS4* and *APGL2* had no difference among the wild-type, OsRac1 knockout and overexpression lines (Figure S10B in Supporting Information). Therefore, FLR1 may regulate grain size and quality through different mechanisms.

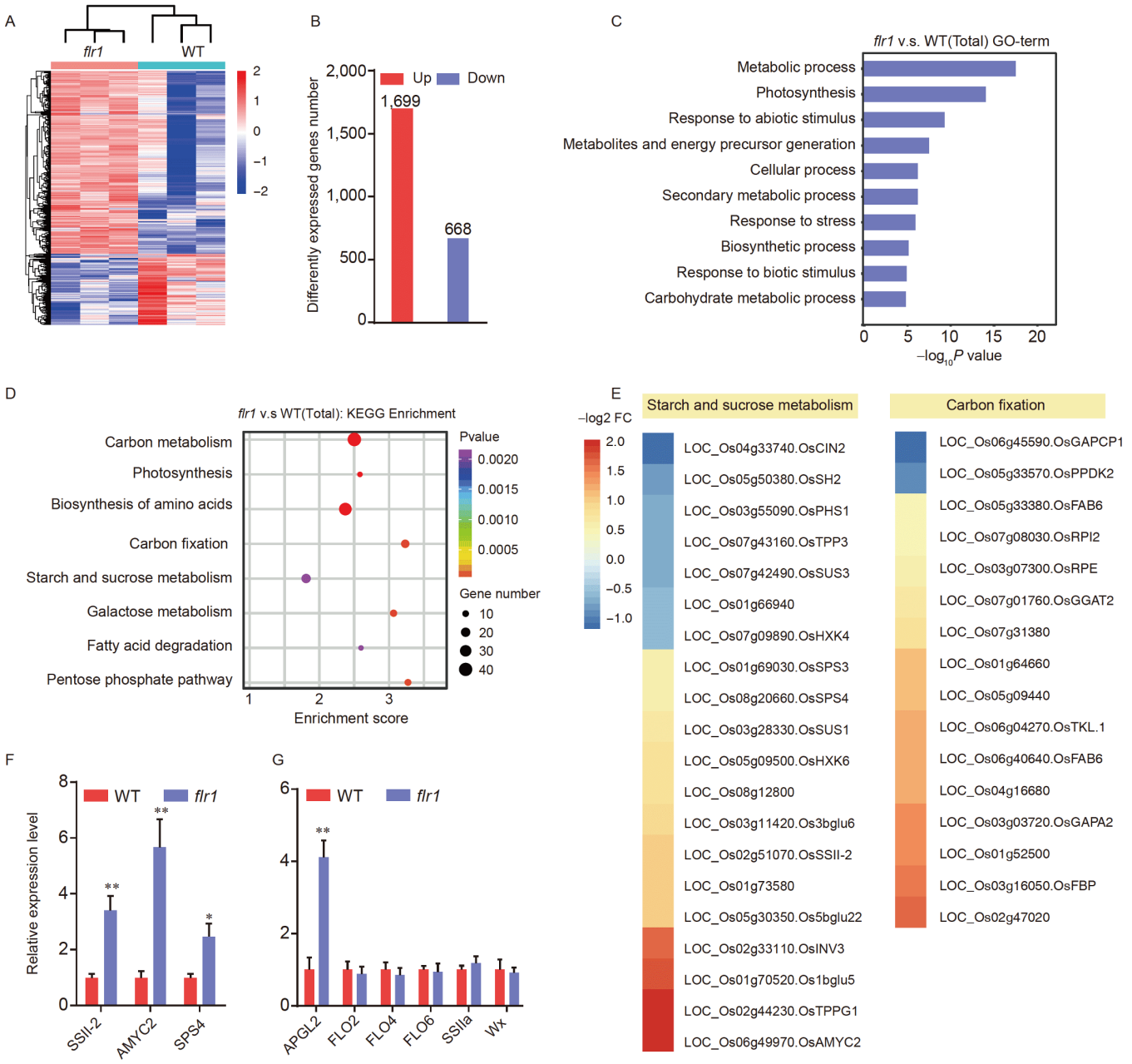

Figure 9 RNA-seq analyses of WT and *flr1* mutant plants. A, A heat map of DEG in WT and *flr1* mutant plants (n=3). Samples (rows) and genes (column) are hierarchically clustered using a Pearson's correlation. B, Summary of DEG with a fold change>1.5 (P<0.05) in the *flr1* mutant. C, Distribution of top 10 biological process GO terms for DEG in the *flr1* mutant. D, KEGG pathways that were enriched in *flr1* mutant DEGs. E, Fold change of DEGs in different KEGG pathways. The color in each cell indicates the value of the log2 fold change (*flr1*/DJ). F and G, Validation of RNA-seq results by qPCR analyses. Experiments were performed using three biological replicates. The error bars represent the SD of three technical replicates. **, P<0.01; one-way ANOVA with Tukey's test.

DISCUSSION

FLR family members are highly conserved in plants and have multiple functions, such as regulating cell growth (Guo et al., 2009; Duan et al., 2010; Mao et al., 2015), modulating fruit ripening in apple and strawberry (Jia et al., 2017a; Jia et al., 2017b), and responding to multiple stress responses in *Arabidopsis* (Yu et al., 2012; Chen et al., 2016; Liao et al., 2017; Zhao et al., 2018; Gong et al., 2020). In this study, we investigated FLR's role in seed development in rice, particularly in determining grain size and grain quality. FLR1 and FLR2 have the highest protein sequence homology to *At*FER from *Arabidopsis* (Figure S1 in Supporting Information), *At*FER regulates setting percentage and seed size in *Arabidopsis* (Escobar-Restrepo et al., 2007; Yu et al., 2014), and FLR1 and FLR2 also regulate setting percentage and seed size in rice, suggesting that the function of *FERs* in fertility and grain size regulation is conserved (Li et al., 2016; Pu et

al., 2017). However, there are notable differences between the functions of *FLR1* and *FLR2*. Previous studies have suggested that FLR1 and FLR2 play different roles in regulating plant height and rice fertility (Li et al., 2016; Pu et al., 2017). In this study, we found that FLR1 primarily affected grain width, while FLR2 affected grain length, supporting the hypothesis that *At*FER differentiated into FLR1 and FLR2 during the divergence of dicotyledons to monocotyledons (Li et al., 2016). Although FLR1 and FLR2 proteins are highly homologous, there are amino acid sequence differences between them in the extracellular domain and kinase domain. The extracellular domain can recognize different ligands to trigger different downstream targets. For example, *At*FER can recruit its chaperones/coreceptors LRE and LLG1 to perceive different RALF peptides, leading to divergent downstream results (Ge et al., 2019; Chen et al., 2020). Specific sites in kinase domains are important for FLRs to interact and phosphorylate downstream targets (Chen et al., 2020). For example, OsRac1 can interact with FLR1 but not with FLR2, which is likely caused by signaling component differences in FLR1 and FLR2, leading to different roles/outputs during grain development.

FLR1 and OsRac1 play opposite roles in regulating grain size. While attempting to elucidate the mechanism by which these proteins regulate grain size, we found that FLR1 preferentially interacted with the active form of OsRac1 and had more activated OsRac1 in the *flr1* mutant compared to the WT, suggesting that FLR1 may bind the more activated OsRac1 on the cell membrane, which would lead to less activated OsRac1 being released from the cell membrane to interact with downstream effectors. Other *FLR* genes (*FLR8* and *FLR15*) also regulate grain size, and we found that *FLR1* and *FLR15* had opposing functions for grain size regulation. Activated OsRac1 can interact with FLR15 but not with FLR1. Obtaining a detailed mechanism of this interaction warrants further study in the future.

We previously found that FER participates in starch accumulation by interacting with GAPC1/2 in *Arabidopsis*. *FER* mutants were found to have abnormal starch accumulation in their leaves (Yang et al., 2015). FER positively regulates protein synthesis by interacting with eIF4E1 (Zhu et al., 2020). In this study, we found that *FLR1* was expressed in several tissues and was also constitutively expressed during endosperm development. This expression pattern suggests that FLR1 is involved in endosperm development. Starch and protein synthesis are the main processes of endosperm development. RNA-seq and qPCR analysis confirmed that FLR1 regulates the expression of starch synthesis genes (*AMYC2*, *APGL2*, *SSII-2*, and *SPS4*) and amino acid biosynthesis. As a result, we found that the starch content increased and that the protein content decreased in *flr1* seeds. This finding prompts the hypothesis that FLR1 may serve as a node of energy metabolism, balancing starch and protein content in rice seeds, and this possibility should be investigated in further studies.

Grain yield and quality are two important traits for improving rice strains, and increasing grain size is one way to improve grain yield. In this study, we found that some FLRs regulate grain size, such as FLR1, FLR2, FLR8 and FLR15, while other FLRs regulate grain quality, such as FLR1, FLR3 and FLR14. FLR1 and FLR15 also regulate plant height and fertility; thus, FLR8 may be a candidate target for breeding programs, as *flr8* mutants have larger grains with similar grain quality as wild type plants. In addition, whether FLRs affect grain yield and quality by interacting with various downstream factors has not been determined. Thus, it is necessary to study the mechanism by identifying the upstream and downstream factors of FLRs to further elucidate how FLRs regulate grain yield and quality.

MATERIALS AND METHODS

Plant materials and growth conditions

Japonica rice cultivars used in this study included Dongjin, Hwayoung (HY), Nipponbare, and T-DNA mutants *flr1* (2C-80049), *flr2* (2D-10654) (Li et al., 2016), *flr* CRISPR-Cas9 lines, lines overexpressing *FLR*, *OsRac1* CRISPR-Cas9 lines and lines overexpressing *OsRac1*. All plants were grown under natural environmental conditions during summer months in the experimental fields of Hunan University, Changsha, China (28°11′N, 112°58′E). All tissues were harvested at Zeitgeber time 3 (ZT 3), and immediately frozen in liquid nitrogen after collection.

Vector construction and transformation of plants

The full length CDS fragments of *FLR1*, *FLR2*, *FLR3*, *FLR8* and *FLR14* were amplified (Innovagene, Changsha, China), and inserted into pCAMBIA1300 with the 35S promoter (Innovagene). The full length CDS fragments of *OsRac1* were amplified and inserted into pCAMBIA1390 with the Ubiquitin promoter and a Flag tag. *FLR1* and *FLR2* recombinant constructs were introduced into *Agrobacterium tumefaciens* strain EHA105, and transfected to rice using the DJ and HY lines, respectively. *OsRac1*, *FLR3*, *FLR8* and *FLR14* recombinant constructs were transfected into the Nipponbare cultivar. Several independent transgenic lines were obtained for each gene, and of these, two independent lines with the highest expression levels were selected for experimental analysis (Figures S1A and S7B in Supporting Information). For CRISPR-Cas9 experiments, CRISPR-GE tool (http://skl.scau.edu.cn/) was used to select two gRNA targets in each *FLR* gene family and to design the primers (Xie et al., 2017). One of the gRNAs was inserted into the pYLgRNA-OsU6a vector, the other was

inserted into the pYLgRNA-OsU6b vector, and both of two gRNA targets were ligated into the Cas9 expression backbone YLCRISPR/Cas9Pubi-H (Ma et al., 2015). pYLCRISPR/Cas9Pubi-H was transformed into *Agrobacterium tumefaciens* EHA105 to infect embryogenic calli of wild-type Nipponbare (Yang et al., 2020). The highest-scoring off-target site was amplified from the genomic DNA of the rice lines that were edited using CRISPR-Cas9, and the PCR products were analyzed by sequencing. The primers that were used to amplify the genomic DNA are listed in Table S3 in Supporting Information.

Construction of the phylogenetic tree

The protein sequences of 16 FLRs from *O. sativa japonica* were obtained from MSU Rice Genome Annotation Project Release 7 (http://rice.plantbiology.msu.edu/). The protein sequences were aligned and a phylogenetic tree based on the Poisson correction methods was constructed using DNAMAN (version 8.0), and phylogenetic tree was optimized using iTol (https://itol.embl.de/itol_account.cgi). Domain predictions were performed by using InterPro (http://www.ebi.ac.uk/interpro/search/sequence/).

Phenotypic analysis

The grain width, grain length, 1,000-grain weight, and chalkiness analysis were measured when plants were completely mature (after DAF 40). Grains from the top part of the panicle were used for phenotypic analyses. At least 150 grains were measured for each sample and measurements were repeated three times. Images of fully filled grains without chaff were taken using Canoscan 5600F (Canon, Japan) and grain size, grain length and grain width were measured using ImageJ (https://imagej.nih.gov/ij/download.html). The chalkiness and level of white-core floury endosperm were obtained using images photographed with a Canon camera with a X-ray film illuminator (PD-HA, Yue hua, Shantou, China). Percentage of grain with chalkiness was determined by counting the number of chalky grains compared to the total number of grains.

Microscopy analysis

SEM of the endosperm was performed as described previously (He et al., 2018). Samples were transversely sectioned, natural dried, sputter coated with gold particles, and imaged using a scanning electron microscope (FEI, USA). The transverse sections of endosperms were stained with I_2/KI and observed using an Olympus BX53 light microscope (He et al., 2018). The images of white-core floury endosperm were photographed using a fluorescence microscope (Nikon, Japan).

Histological analysis

Histological analysis was performed as described previously (Kim et al., 2014). Briefly, young spikelet hulls were fixed in FAA (70% ethanol, 5% formaldehyde, 5% glacial acetic acid) for 48 h. Fixed sample were then dehydrated with a gradient of ethanol (70%, 80%, 90%, 100%), and cleared in a xylene series. The thick cross section were cut with a microtome, stained with toluidine blue, and observed under a microscope (Nikon).

Protein extraction and western blot analysis

To analyze the FLR1 protein levels in rice, we harvested three-month-old Dongjin plant tissue and endosperm at different DAF stages, and 100 mg of each tissue was ground into powder in liquid nitrogen and extracted using a RIPA buffer (Beyotime, Shanghai) for 30 min. Protein samples were boiled in 4×SDS loading buffer and centrifuged for 10 min at 12,000×*g*. The supernatant was used for western blot analysis using 10.0% SDS-PAGE. Gels were incubated with the FLR1 antibody (1:1,000) and the bands were detected using ECL (Thermo Fisher Scientific, USA). Anti-GAPDH (abcam, UK) was used as the loading control.

Construction of Y2H library and assays

Total RNA was isolated from young panicles and seedling of Nipponbare using Trizol Reagent (TaKaRa, Japan), and cDNA was synthesized using cDNA synthesis kit (TaKaRa). cDNA library for a Y2H analysis was amplified by long distance PCR (Clontech, Japan) purified after proteinase K digestion, and 3 μg of pGADT7 vector and 4 μg of homogenized and purified double-stranded cDNA were used to co-transform yeast competent cell AH109 with the Yeastmaker Yeast Transformation System 2 protocol (Clontech).

The coding regions for the kinase domains of FLR1 (482–893 aa), FLR2 (481–896 aa), FLR8 (500–844 aa), and FLR15 (520–859 aa) were cloned into the pGBKT7 (BD) vector. FLR1-BD was used as bait in two-hybrid screen of the cDNA library. Briefly, FLR1-BD and the cDNA library were co-transformed into AH109 yeast cells. Then, the transformed cells were plated on synthetic dropout selection medium that did not contain Trp, Leu, and His and supplemented with 20 mmol L^{-1} 3-AT to inhibit self-activation. To confirm the interaction between FLRs and OsRac1, we cloned full length OsRac1, CA-OsRac1 (G19V), DN-OsRac1 (T24N) into pGADT7 vector and co-transformed them into yeast with FLR1-BD, FLR2-BD, FLR8-BD and FLR15-BD into yeast.

Co-IP analyses in HEK293T cells

Human embryonic kidney (HEK) 293T cells were cultured in DMEM medium with 10% (v/v) FBS and 100 mg L^{-1} streptomycin at 37°C in 5% CO_2. The full-length coding sequences of FLR1 were cloned into the pCMV pEGFP-N1 vector to generate GFP-tagged versions of FLR proteins. The full length coding sequence of OsRac1 was cloned into pCMV pTriEX4-Flag. HEK293T were seeded at a density of approximately 3×10^5 per plate, and transfecting 3 μg OsRac1-pTriEX4-Flag with FER-pEGFP-N1 into HEK293 Cells using Lipofectamine 2000 (Thermo Fisher Scientific). Medium was replaced 6 h after transfection, and cells were harvested for Co-IP after 48 h of culturing.

For the Co-IP experiment, 293T cells were washed with PBS and lysed in 500 μL NP 40 Lysis buffer (AMRESCO, USA) with 1% Protease inhibitor cocktail and 1 mmol L^{-1} PMSF. The lysate was placed on ice for 1 h, and centrifuged at 4°C for 10 min. The supernatant was mixed with 25 μL anti-FLAG beads (Bimake, USA) overnight at 4°C. The beads were pelleted and washed three times with washing buffer (20 mmol L^{-1} Tris-HCl, pH 8.0, 150 mmol L^{-1} NaCl, 0.5% NP-40). The beads were boiled with 2×SDS loading buffer at 95°C for 10 min, and the supernatant was collected for SDS-PAGE analysis. FLR1-GFP protein was detected using an antibody against GFP (1:3,000; CMCTAG, AT0028, USA), and OsRac1-Flag protein was detected using the Flag antibody (1:4,000; Abmart, Shanghai, China).

Co-IP analyses in plants

The Co-IP analysis was performed as previously described (Wang et al., 2020b). Briefly, young 3 cm panicles (*OsRac1-OE* transgenic and wild-type) were ground in liquid nitrogen, and frozen powder was extracted with NEB buffer (20 mmol L^{-1} HEPES-KOH (pH 7.5), 40 mmol L^{-1} KCl, 1 mmol L^{-1} EDTA, 1 mmol L^{-1} PMSF and protease inhibitor (Thermo Fisher Scientific)) and NEB-T buffer (NEB buffer containing 1% Triton X-100) for 1 h at 4°C. Anti-Flag bead (Bimake) were used for enriching flag-tagged protein, anti-FLAG (1:4,000; Abmart) and anti-FLR1 antibodies (1:1,000) were used in WB analyses.

Pull down analyses

Pull down assays were performed as described (Wang et al., 2020b). FLR1-MBP (482–893 aa), MBP and His-OsRac1 were expressed in *E. coli* BL21 by IPTG (0.5 mmol L^{-1}) induction. His-OsRac1 and FLR1-MBP/MBP were purified following standard protocols. His-OsRac1 and FLR1-MBP were then coincubated with 30 μL MBP resin (Sangon Biotech, Shanghai) in binding buffer (20 mmol L^{-1} Tris-HCl (pH 8.0) 150 mmol L^{-1} NaCl, and 1 mmol L^{-1} EDTA) with GTP or GDP at 4°C for 6 h. After incubation, the resin was washed with washing buffer 1 (20 mmol L^{-1} Tris-HCl (pH 8.0), 300 mmol L^{-1} NaCl, and 0.5% Triton X-100) for 10 min, washing buffer 2 (20 mmol L^{-1} Tris-HCl (pH 8.0), 300 mmol L^{-1} NaCl, and 1 mmol L^{-1} EDTA) for 10 min. After the final washing, loading buffer was added, and the suspension was heated at 95°C for 10 min. SDS-PAGE, immunoblotting and CBB were performed according to standard protocols.

OsRac1 activity analysis

For AtRIC1 pull down of activated OsRac1, GST-AtRIC1 and GST protein were expressed in *E. coli* BL21 by IPTG (0.5 mmol L^{-1}) induction. Young 3 cm (0.15 g) panicles were ground in liquid nitrogen, and frozen powder was extracted in binding buffer (50 mmol L^{-1} Tris-HCl (pH 7.5), 150 mmol L^{-1} NaCl, 0.3% Triton X-100, 1 mmol L^{-1} PMSF, and protease inhibitor (Thermo Fisher Scientific)) for 30 min. 300 μL supernatant and 20 μL GST-AtRIC1 protein were applied to GST-AtRIC1 resin for pull down assays; 40 μL supernatant was saved for protein quantification. After incubation, the resin was washed with washing buffer 1 (50 mmol L^{-1} Tris-HCl (pH 8.0), 150 mmol L^{-1} NaCl, and 0.5% Triton X-100) for 10 min, washing buffer 2 (50 mmol L^{-1} Tris-HCl (pH 8.0), 200 mmol L^{-1} NaCl, and 1 mmol L^{-1} EDTA) for 10 min. After the final wash, the resin was eluted in SDS/PAGE loading buffer, boiled for 5 min at 95°C, and applied to 12% SDS/PAGE for protein blot analysis. OsRac1 antibody (1:2,000; Abiocode, USA) was used to detect OsRac1 protein level, and GST antibody (1:5,000; CMC) was used to detect the GST protein.

Measurements of total starch, amylose and protein content

Fully filled seeds were ground into a powder to measure starch and amylose content. Total starch content was detected using the dinitrosalicylic acid colorimetric method (DNS method). Briefly, 50 mg of rice endosperm powder was mixed with 6 mL 2.5 mol L^{-1} KOH (40°C) to gelatinize the sample, and the mixture was shaken vigorously for 5 min. The sample was then mixed with 3 mL 0.4 mol L^{-1} NaAc (pH 4.75), and adjusted the pH to 4.75 using HCl. Finally, 60 μL glucosaccharase was added to the incubating mixture at 60°C for 45 min, and centrifuged at 5,000×*g* for 2 min at 4°C. Absorbance at 540 nm was measured, and the total starch content determined by comparing the absorbance to a calibration curve prepared using soluble starch standards. The amylose content was measured using concanavalin A (Con A), as described previously (Gibson et al., 1997). Standard amylose samples were purchased from Sigma-Aldrich (USA). The total protein content was mea-

sured using an XDS Near-Infrared Rapid Content Analyzer with near-infrared reflectance spectroscopy, as previously described (Perbandt et al., 2010). RVA were conducted using 3 g rice powder (0.5 mm, 14% misture basis) mixed with 25 mL of distilled water, then measured by a Rapid Visco Analyzer (RVA Techmaster, Newport Scientific SUper4, Australia) following the National Standard Code for Chinese characters GB/T 24852-2010.

Histochemical GUS assays

To generate the GUS reporter vector driven by the *FLR1* promoter, we cloned the 1,602 bp promoter sequence of *FLR1* upstream of GUS into the pCAMBIA1301 vector. The recombined vector was transformed into Nipponbare using *Agrobacterium tumefaciens*. The transgenic plants from the T1 generation were used for GUS staining. Briefly, samples were vacuumed for 30 min, placed in staining solution (Huayueyang, Beijing, China) for 12 h at 37°C, and washed using 75% ethanol. The stained tissues were imaged using a Canon camera.

Purification of GST-tag proteins and preparation of FLR1 antibody

The N-terminal region (1–450 aa) of FLR1 was amplified and cloned into pGEX4T-1 to generate GST-tagged FLR1, which was induced in *E. coli* strain BL21 at 16°C for 16 h. GST-tagged FLR1 was purified using methods described in the manual of Pierce Glutathione Agarose (Thermo Fisher Scientific). To produce the FLR1 antibody, we emulsified 100 μg purified GST-FLR1 protein with Complete Freund's adjuvant (Sigma-Aldrich) and injected it into a 45-day SPF male SD rat. 100 μg purified GST-FLR1 protein was emulsified with Incomplete Freund's adjuvant (Sigma-Aldrich) and injected into the same rat next week. The injection was repeated three times. Blood was sampled from the rat's eyes and serum was obtained by centrifugation of the blood at 12,000×*g* for 10 min. Effectiveness of the antibody was validated using western blot analyses using protein extracts from WT (Dongjin) and *flr1*.

RNA-seq analyses

Dongjin and *flr1* plants grown under natural environment for three months and the grains at the DAF 12 stage were collected for total RNA extraction. Total RNA was extracted using the mirVana miRNA Isolation Kit (Thermo Fisher Scientific). RNA integrity number (RIN) ≥7 were subjected to the subsequent analyses. We used TruSeq Stranded mRNA LT Sample Prep Kit (Illumina, USA) to construct the libraries according to the manufacturer's instructions. Illumina sequencing was performed with OE biotech Co., Ltd. (Shanghai).

Raw data (raw reads) were processed by using the Trimmomatic with the parameters "CROP:150 ILLUMINACLIP: TruSeq3-PE-2.fa:2:30:10:8:true LEADING:3 TRAILING:3 SLIDINGWINDOW:4:15 MINLEN:50" (http://www.usadellab.org/cms/?page=trimmomatic) (Bolger et al., 2014). Reads were mapped to the Os-Nipponbare-Reference-IRGSP-1.0 pseudomolecules using hisat2 (https://ccb.jhu.edu/software/hisat2/index.shtml) (Kim et al., 2015). The FPKM value of each gene was calculated using cufflinks (Roberts et al., 2011), and the read counts of each gene were obtained by htseq-count (Anders et al., 2015). DEGs were identified using the DESeq (2012) R package functions estimateSizeFactors and nbinomTest. P value <0.05 and fold change >1.5 or fold change <0.5 were set as the threshold for significantly differential expression. Hierarchical cluster analysis of DEGs was performed to explore gene expression patterns. GO enrichment and KEGG (Kanehisa et al., 2008) pathway enrichment analyses of DEGs were respectively performed using R based on the hypergeometric distribution. The raw RNA-seq data were uploaded to the NCBI database with the accession number SRX6849320.

RNA extraction and qPCR analyses

Young panicles that were 3 cm long and grains at DAF 12 stage were harvested for RNA extraction using the TRIzol reagent (TaKaRa). cDNA was synthesized from 500 ng of total RNA by using the Fermentas cDNA synthesis kit (Fermentas, USA). qPCR was performed on a Bio-RAD thermocycler with SYBR Premix *Ex* Taq II (TaKaRa). The cDNAs were amplified following denaturation using 40-cycle programs (95°C, 15 s; 60°C, 20 s per cycle). *OsACTIN* was used as an internal control.

Statistics

Any significant differences in data were analyzed by Student's *t*-test or by multivariate comparison (one-way ANOVA) using SPSS (version 17.0) software. All statistical tests were described in the figure legends and/or in the Materials and Methods section.

Compliance and ethics *The author(s) declare that they have no conflict of interest.*

Acknowledgements *This work was supported by the National Natural Science Foundation of China (NSFC-31571444, 31400232, 31571874), China Postdoctoral Science Foundation (2019M662763) and the Open Research Fund of State Key Laboratory of Hybrid Rice (Hunan Hybrid Rice Research Center) (2020KF02).*

References

Akamatsu, A., Wong, H.L., Fujiwara, M., Okuda, J., Nishide, K., Uno, K., Imai, K., Umemura, K., Kawasaki, T., Kawano, Y., et al. (2013). An

OsCEBiP/OsCERK1-OsRacGEF1-OsRac1 module is an essential early component of chitin-induced rice immunity. Cell Host Microbe 13, 465–476.
Anders, S., Pyl, P.T., and Huber, W. (2015). HTSeq—A Python framework to work with high-throughput sequencing data. Bioinformatics 31, 166–169.
Bolger, A.M., Lohse, M., and Usadel, B. (2014). Trimmomatic: a flexible trimmer for Illumina sequence data. Bioinformatics 30, 2114–2120.
Chen, J., Yu, F., Liu, Y., Du, C., Li, X., Zhu, S., Wang, X., Lan, W., Rodriguez, P.L., Liu, X., et al. (2016). FERONIA interacts with ABI2-type phosphatases to facilitate signaling cross-talk between abscisic acid and RALF peptide in *Arabidopsis*. Proc Natl Acad Sci USA 113, E5519–E5527.
Chen, J., Zhu, S., Ming, Z., Liu, X., and Yu, F. (2020). FERONIA cytoplasmic domain: node of varied signal outputs. aBIOTECH 1, 135–146.
Duan, Q., Kita, D., Li, C., Cheung, A.Y., and Wu, H.M. (2010). FERONIA receptor-like kinase regulates RHO GTPase signaling of root hair development. Proc Natl Acad Sci USA 107, 17821–17826.
Escobar-Restrepo, J.M., Huck, N., Kessler, S., Gagliardini, V., Gheyselinck, J., Yang, W.C., and Grossniklaus, U. (2007). The FERONIA receptor-like kinase mediates male-female interactions during pollen tube reception. Science 317, 656–660.
Ge, Z., Dresselhaus, T., and Qu, L.J. (2019). How CrRLK1L receptor complexes perceive RALF signals. Trends Plant Sci 24, 978–981.
Gibson, T.S., Solah, V.A., and McCleary, B.V. (1997). A procedure to measure amylose in cereal starches and flours with concanavalin A. J Cereal Sci 25, 111–119.
Gong, Z., Xiong, L., Shi, H., Yang, S., Herrera-Estrella, L.R., Xu, G., Chao, D.Y., Li, J., Wang, P.Y., Qin, F., et al. (2020). Plant abiotic stress response and nutrient use efficiency. Sci China Life Sci 63, 635–674.
Guo, H., Li, L., Ye, H., Yu, X., Algreen, A., and Yin, Y. (2009). Three related receptor-like kinases are required for optimal cell elongation in *Arabidopsis thaliana*. Proc Natl Acad Sci USA 106, 7648–7653.
Guo, T., Chen, K., Dong, N.Q., Shi, C.L., Ye, W.W., Gao, J.P., Shan, J.X., and Lin, H.X. (2018). *GRAIN SIZE AND NUMBER1* negatively regulates the OsMKKK10-OsMKK4-OsMPK6 cascade to coordinate the trade-off between grain number per panicle and grain size in rice. Plant Cell 30, 871–888.
Hannah, L.C., and James, M. (2008). The complexities of starch biosynthesis in cereal endosperms. Curr Opin Biotech 19, 160–165.
Haruta, M., Sabat, G., Stecker, K., Minkoff, B.B., and Sussman, M.R. (2014). A peptide hormone and its receptor protein kinase regulate plant cell expansion. Science 343, 408–411.
He, W., Lin, L., Wang, J., Zhang, L., Liu, Q., and Wei, C. (2018). Inhibition of starch branching enzymes in waxy rice increases the proportion of long branch-chains of amylopectin resulting in the comb-like profiles of starch granules. Plant Sci 277, 177–187.
Hirose, T., and Terao, T. (2004). A comprehensive expression analysis of the starch synthase gene family in rice (*Oryza sativa* L.). Planta 220, 9–16.
Huang, Y.Y., Liu, X.X., Xie, Y., Lin, X.Y., Hu, Z.J., Wang, H., Wang, L.F., Dang, W.Q., Zhang, L.L., Zhu, Y., et al. (2020). Identification of *FERONIA-like receptor* genes involved in rice-*Magnaporthe oryzae* interaction. Phytopathol Res 2, 14.
Jia, M., Ding, N., Zhang, Q., Xing, S., Wei, L., Zhao, Y., Du, P., Mao, W., Li, J., Li, B., et al. (2017a). A FERONIA-like receptor kinase regulates strawberry (*Fragaria×ananassa*) fruit ripening and quality formation. Front Plant Sci 8, 1099.
Jia, M., Du, P., Ding, N., Zhang, Q., Xing, S., Wei, L., Zhao, Y., Mao, W., Li, J., Li, B., et al. (2017b). Two FERONIA-like receptor kinases regulate apple fruit ripening by modulating ethylene production. Front Plant Sci 8, 1406.
Kanehisa, M., Araki, M., Goto, S., Hattori, M., Hirakawa, M., Itoh, M., Katayama, T., Kawashima, S., Okuda, S., Tokimatsu, T., et al. (2008). KEGG for linking genomes to life and the environment. Nucleic Acids Res 36, D480–D484.
Kawano, Y., Akamatsu, A., Hayashi, K., Housen, Y., Okuda, J., Yao, A., Nakashima, A., Takahashi, H., Yoshida, H., Wong, H.L., et al. (2010). Activation of a Rac GTPase by the NLR family disease resistance protein Pit plays a critical role in rice innate immunity. Cell Host Microbe 7, 362–375.
Kim, D.M., Lee, H.S., Kwon, S.J., Fabreag, M.E., Kang, J.W., Yun, Y.T., Chung, C.T., and Ahn, S.N. (2014). High-density mapping of quantitative trait loci for grain-weight and spikelet number in rice. Rice 7, 14.
Kim, D., Langmead, B., and Salzberg, S.L. (2015). HISAT: a fast spliced aligner with low memory requirements. Nat Methods 12, 357–360.
Li, C., Wang, L., Cui, Y., He, L., Qi, Y., Zhang, J., Lin, J., Liao, H., Lin, Q., Yang, T., et al. (2016). Two *FERONIA-like receptor* (*FLR*) genes are required to maintain architecture, fertility, and seed yield in rice. Mol Breeding 36, 151.
Li, N., Xu, R., and Li, Y. (2019). Molecular networks of seed size control in plants. Annu Rev Plant Biol 70, 435–463.
Liao, H., Tang, R., Zhang, X., Luan, S., and Yu, F. (2017). FERONIA receptor kinase at the crossroads of hormone signaling and stress responses. Plant Cell Physiol 58, 1143–1150.
Liu, L., Zheng, C., Kuang, B., Wei, L., Yan, L., and Wang, T. (2016). Receptor-like kinase RUPO interacts with potassium transporters to regulate pollen tube growth and integrity in rice. PLoS Genet 12, e1006085.
Luo, X., and Liu, J. (2018). Insights into receptor-like kinases-activated downstream events in plants. Sci China Life Sci 61, 1586–1588.
Ma, X., Zhang, Q., Zhu, Q., Liu, W., Chen, Y., Qiu, R., Wang, B., Yang, Z., Li, H., Lin, Y., et al. (2015). A robust CRISPR/Cas9 system for convenient, high-efficiency multiplex genome editing in monocot and dicot plants. Mol Plant 8, 1274–1284.
Mao, D., Yu, F., Li, J., Van de Poel, B., Tan, D., Li, J., Liu, Y., Li, X., Dong, M., Chen, L., et al. (2015). FERONIA receptor kinase interacts with *S*-adenosylmethionine synthetase and suppresses *S*-adenosylmethionine production and ethylene biosynthesis in *Arabidopsis*. Plant Cell Environ 38, 2566–2574.
Morris, E.R., and Walker, J.C. (2003). Receptor-like protein kinases: the keys to response. Curr Opin Plant Biol 6, 339–342.
Nakamura, Y. (2018). Rice starch biotechnology: rice endosperm as a model of cereal endosperms. Starch 70, 1600375.
Nguyen, Q.N., Lee, Y.S., Cho, L.H., Jeong, H.J., An, G., and Jung, K.H. (2015). Genome-wide identification and analysis of *Catharanthus roseus* RLK1-like kinases in rice. Planta 241, 603–613.
Nissen, K.S., Willats, W.G.T., and Malinovsky, F.G. (2016). Understanding CrRLK1L function: cell walls and growth control. Trends Plant Sci 21, 516–527.
Peng, C., Wang, Y., Liu, F., Ren, Y., Zhou, K., Lv, J., Zheng, M., Zhao, S., Zhang, L., Wang, C., et al. (2014). *FLOURY ENDOSPERM6* encodes a CBM48 domain-containing protein involved in compound granule formation and starch synthesis in rice endosperm. Plant J 77, 917–930.
Perbandt, D., Reulein, J., Richter, F., Stülpnagel, R., and Wachendorf, M. (2010). Assessment of mass flows and fuel quality during mechanical dehydration of silages using near infrared reflectance spectroscopy. Bioenerg Res 3, 194–203.
Pu, C.X., Han, Y.F., Zhu, S., Song, F.Y., Zhao, Y., Wang, C.Y., Zhang, Y.C., Yang, Q., Wang, J., Bu, S.L., et al. (2017). The rice receptor-like kinases DWARF AND RUNTISH SPIKELET1 and 2 repress cell death and affect sugar utilization during reproductive development. Plant Cell 29, 70–89.
Roberts, A., Trapnell, C., Donaghey, J., Rinn, J.L., and Pachter, L. (2011). Improving RNA-Seq expression estimates by correcting for fragment bias. Genome Biol 12, R22.
Sakamoto, T., and Matsuoka, M. (2008). Identifying and exploiting grain yield genes in rice. Curr Opin Plant Biol 11, 209–214.
Schulze-Muth, P., Irmler, S., Schröder, G., and Schröder, J. (1996). Novel type of receptor-like protein kinase from a higher plant (*Catharanthus roseus*). J Biol Chem 271, 26684–26689.

Shafie, B., Cheng, S., Lee, H., Yiu, P. (2016). Characterization and classification of whole-grain rice based on rapid visco analyzer (RVA) pasting profile. Int Food Res J 23, 2138–2143.
She, K.C., Kusano, H., Koizumi, K., Yamakawa, H., Hakata, M., Imamura, T., Fukuda, M., Naito, N., Tsurumaki, Y., Yaeshima, M., et al. (2010). A novel factor *FLOURY ENDOSPERM2* is involved in regulation of rice grain size and starch quality. Plant Cell 22, 3280–3294.
Stegmann, M., Monaghan, J., Smakowska-Luzan, E., Rovenich, H., Lehner, A., Holton, N., Belkhadir, Y., and Zipfel, C. (2017). The receptor kinase FER is a RALF-regulated scaffold controlling plant immune signaling. Science 355, 287–289.
Wang, Q., Zuo, Z., Wang, X., Gu, L., Yoshizumi, T., Yang, Z., Yang, L., Liu, Q., Liu, W., Han, Y.J., et al. (2016). Photoactivation and inactivation of *Arabidopsis* cryptochrome 2. Science 354, 343–347.
Wang, L., Yang, T., Lin, Q., Wang, B., Li, X., Luan, S., and Yu, F. (2020a). Receptor kinase FERONIA regulates flowering time in *Arabidopsis*. BMC Plant Biol 20, 26.
Wang, L., Yang, T., Wang, B., Lin, Q., Zhu, S., Li, C., Ma, Y., Tang, J., Xing, J., Li, X., et al. (2020b). RALF1-FERONIA complex affects splicing dynamics to modulate stress responses and growth in plants. Sci Adv 6, eaaz1622.
Xie, X., Ma, X., Zhu, Q., Zeng, D., Li, G., and Liu, Y.G. (2017). CRISPR-GE: A convenient software toolkit for CRISPR-based genome editing. Mol Plant 10, 1246–1249.
Xiao, Y., Stegmann, M., Han, Z., DeFalco, T.A., Parys, K., Xu, L., Belkhadir, Y., Zipfel, C., and Chai, J. (2019). Mechanisms of RALF peptide perception by a heterotypic receptor complex. Nature 572, 270–274.
Xu, G., Chen, W., Song, L., Chen, Q., Zhang, H., Liao, H., Zhao, G., Lin, F., Zhou, H., and Yu, F. (2019). FERONIA phosphorylates E3 ubiquitin ligase ATL6 to modulate the stability of 14-3-3 proteins in response to the carbon/nitrogen ratio. J Exp Bot 70, 6375–6388.
Xu, J., and Zhang, S. (2015). Mitogen-activated protein kinase cascades in signaling plant growth and development. Trends Plant Sci 20, 56–64.
Xu, R., Duan, P., Yu, H., Zhou, Z., Zhang, B., Wang, R., Li, J., Zhang, G., Zhuang, S., Lyu, J., et al. (2018). Control of grain size and weight by the OsMKKK10-OsMKK4-OsMAPK6 signaling pathway in rice. Mol Plant 11, 860–873.
Yang, T., Wang, L., Li, C., Liu, Y., Zhu, S., Qi, Y., Liu, X., Lin, Q., Luan, S., and Yu, F. (2015). Receptor protein kinase FERONIA controls leaf starch accumulation by interacting with glyceraldehyde-3-phosphate dehydrogenase. Biochem Biophys Res Commun 465, 77–82.
Yang, Z., Xing, J., Wang, L., Liu, Y., Qu, J., Tan, Y., Fu, X., Lin, Q., Deng, H., and Yu, F. (2020). Mutations of two *FERONIA-like receptor* genes enhance rice blast resistance without growth penalty. J Exp Bot 71, 2112–2126.
Yang, Z., and Fu, Y. (2007). ROP/RAC GTPase signaling. Curr Opin Plant Biol 10, 490–494.
Yu, F., Qian, L., Nibau, C., Duan, Q., Kita, D., Levasseur, K., Li, X., Lu, C., Li, H., Hou, C., et al. (2012). FERONIA receptor kinase pathway suppresses abscisic acid signaling in *Arabidopsis* by activating ABI2 phosphatase. Proc Natl Acad Sci USA 109, 14693–14698.
Yu, F., Li, J., Huang, Y., Liu, L., Li, D., Chen, L., and Luan, S. (2014). FERONIA receptor kinase controls seed size in *Arabidopsis thaliana*. Mol Plant 7, 920–922.
Yu, X., Xia, S., Xu, Q., Cui, Y., Gong, M., Zeng, D., Zhang, Q., Shen, L., Jiao, G., Gao, Z., et al. (2020). *ABNORMAL FLOWER AND GRAIN 1* encodes OsMADS6 and determines palea identity and affects rice grain yield and quality. Sci China Life Sci 63, 228–238.
Zhang, Q. (2007). Strategies for developing Green Super Rice. Proc Natl Acad Sci USA 104, 16402–16409.
Zhang, G., Cheng, Z., Zhang, X., Guo, X., Su, N., Jiang, L., Mao, L., and Wan, J. (2011). Double repression of soluble starch synthase genes *SSIIa* and *SSIIIa* in rice (*Oryza sativa* L.) uncovers interactive effects on the physicochemical properties of starch. Genome 54, 448–459.
Zhang, L., Ren, Y., Lu, B., Yang, C., Feng, Z., Liu, Z., Chen, J., Ma, W., Wang, Y., Yu, X., et al. (2016). *FLOURY ENDOSPERM7* encodes a regulator of starch synthesis and amyloplast development essential for peripheral endosperm development in rice. J Exp Bot 67, 633–647.
Zhang, Y., Xiong, Y., Liu, R., Xue, H.W., and Yang, Z. (2019). The Rho-family GTPase *OsRac1* controls rice grain size and yield by regulating cell division. Proc Natl Acad Sci USA 116, 16121–16126.
Zhao, C., Zayed, O., Yu, Z., Jiang, W., Zhu, P., Hsu, C.C., Zhang, L., Tao, W.A., Lozano-Durán, R., and Zhu, J.K. (2018). Leucine-rich repeat extensin proteins regulate plant salt tolerance in *Arabidopsis*. Proc Natl Acad Sci USA 115, 13123–13128.
Zhu, S., Estévez, J.M., Liao, H., Zhu, Y., Yang, T., Li, C., Wang, Y., Li, L., Liu, X., Pacheco, J.M., et al. (2020). The RALF1-FERONIA complex phosphorylates eIF4E1 to promote protein synthesis and polar root hair growth. Mol Plant 13, 698–716.

SUPPORTING INFORMATION

The supporting information is available online at https://doi.org/10.1007/s11427-020-1780-x. The supporting materials are published as submitted, without typesetting or editing. The responsibility for scientific accuracy and content remains entirely with the authors.